Explosion and Final State of an Unstable Reissner-Nordström Black Hole

Nicolas Sanchis-Gual,[1] Juan Carlos Degollado,[2,3] Pedro J. Montero,[4] José A. Font,[1,5] and Carlos Herdeiro[6]
[1]Departamento de Astronomía y Astrofísica, Universitat de València, Doctor Moliner 50, 46100, Burjassot (València), Spain
[2]Instituto de Ciencias Físicas, Universidad Nacional Autónoma de México, Apartado Postal 48-3, 62251 Cuernavaca, Morelos, México
[3]Departamento de Ciencias Computacionales, Centro Universitario de Ciencias Exactas e Ingeniería, Universidad de Guadalajara Avenida Revolución 1500, Colonia Olímpica C.P. 44430 Guadalajara, Jalisco, Mexico
[4]Max-Planck-Institut für Astrophysik, Karl-Schwarzschild-Strasse 1, 85748 Garching bei München, Germany
[5]Observatori Astronòmic, Universitat de València, C/ Catedrático José Beltrán 2, 46980 Paterna (València), Spain
[6]Departamento de Física da Universidade de Aveiro and CIDMA, Campus de Santiago, 3810-183 Aveiro, Portugal
(Received 22 December 2015; revised manuscript received 26 February 2016; published 7 April 2016)

A Reissner-Nordström black hole (BH) is superradiantly unstable against spherical perturbations of a charged scalar field enclosed in a cavity, with a frequency lower than a critical value. We use numerical relativity techniques to follow the development of this unstable system—dubbed *a charged BH bomb*—into the nonlinear regime, solving the full Einstein-Maxwell-Klein-Gordon equations, in spherical symmetry. We show that (i) the process stops before all the charge is extracted from the BH, and (ii) the system settles down into a hairy BH: a charged horizon in equilibrium with a scalar field condensate, whose phase is oscillating at the (final) critical frequency. For a low scalar field charge q, the final state is approached smoothly and monotonically. For large q, however, the energy extraction overshoots, and an explosive phenomenon, akin to a *bosenova*, pushes some energy back into the BH. The charge extraction, by contrast, does not reverse.

DOI: 10.1103/PhysRevLett.116.141101

Introduction.—A remarkable feature of rotating (Kerr) black holes (BHs) is that they may, classically, give away energy and angular momentum. A bosonic field can be the extraction mediator. Its waves, with sufficiently slowly rotating phases, are amplified when scattering off a corotating BH [1–9]. Trapping these *superradiantly scattered* waves around the BH, the bosonic field piles up exponentially into a gravitating macroscopic Bose-Einstein-type condensate. It has been conjectured that an explosive phenomenon ensues, dubbed *a BH bomb* [3]. Understanding the explosion and final state of the BH bomb has been an open issue since the 1970s [10].

The BH bomb proposal was based on linear studies of the superradiant instability. The conjectured explosive regime, however, is nonlinear, and numerical evolutions using the full Einstein equations are mandatory to probe it. Unfortunately, the growth rates of superradiant instabilities for rotating BHs are too small [7,11], rendering the numerical evolution of the rotating BH bomb a *tour de force* with current numerical relativity (NR) technology [12,13]. But suggestive progress has come from two other types of nonlinear studies. First, considering a test bosonic field with nonlinear dynamics on the Kerr BH [14,15] produced evidence that an explosive event indeed occurs, akin to the *bosenova* observed in condensed matter systems [16]. Second, *hairy BH* solutions with a stationary geometry of the fully nonlinear Einstein-bosonic field system were found precisely at the threshold of the instability [17,18].

In the absence of the NR technology to address the rotating BH bomb, we are led to the more favorable situation that occurs for charged (Reissner-Nordström) BHs. An analogue process to superradiant scattering can take place, by which Coulomb energy and charge are extracted from the BH by a *charged* bosonic field [19,20]. This occurs for sufficiently small frequency waves and for a field with the same charge (sign) as the BH. Introducing a trapping mechanism, a *charged BH bomb* forms. On the one hand, linear studies show that the growth rates of such charged superradiant instability can be much larger than for their rotating counterparts [21–23]. On the other hand, the instability can occur within spherical symmetry, in contrast with the rotating case that breaks even axial symmetry. These features make the study of the charged BH bomb amenable with current NR techniques.

In this Letter, we report NR simulations, using the full Einstein equations, of the charged BH bomb. As a simple model, we take a charged scalar field (SF) as the bosonic mediator and enclose the BH-SF system in a cavity, as a trapping mechanism. We find that the nonlinear regime may be, albeit needs not be, explosive. Moreover, we establish that, regardless of how explosive the nonlinear regime is, the generic final state is a *hairy* BH: a charged horizon surrounded by a SF condensate storing part of the charge and energy of the initial BH and with a phase oscillating at the threshold frequency of the superradiant instability. Hairy BHs of this sort have been recently constructed and shown to be stable [24].

Framework.—We consider the Einstein-Maxwell-Klein-Gordon (EMKG) system described by the action $\mathcal{S} = \int d^4x\sqrt{-g}\mathcal{L}$, with Lagrangian density

$$\mathcal{L} = \frac{R - F_{\alpha\beta}F^{\alpha\beta}}{16\pi} - \frac{1}{2}D_\alpha\Phi(D^\alpha\Phi)^* - \frac{\mu^2}{2}|\Phi|^2, \quad (1)$$

where R is the Ricci scalar, $F_{\alpha\beta} \equiv \nabla_\alpha A_\beta - \nabla_\beta A_\alpha$, A_α is the electromagnetic potential, D_α is the gauge covariant derivative, $D_\alpha \equiv \nabla_\alpha - iqA_\alpha$, and q and μ are the charge and the mass of the scalar field. Newton's constant, the speed of light, and $4\pi\epsilon_0$ are set to 1 in our units.

To address numerically the EMKG system, we use a generalized BSSN formulation [25,26] adapted to spherical symmetry [27–29], and the code described in Refs. [30,31]. This code was upgraded to account for Maxwell's equations and energy-momentum tensor. The $3+1$ metric split reads $ds^2 = -(\alpha^2 + \beta^r\beta_r)dt^2 + 2\beta_r dtdr + e^{4\chi}[adr^2 + br^2 d\Omega_2]$, where the lapse α, shift component β^r, and the (spatial) metric functions χ, a, b depend on t, r. The electric field $E^\mu = F^{\mu\nu}n_\nu$ has only a radial component, and the magnetic field $B^\mu = \star F^{\mu\nu}n_\nu$ vanishes, where n^μ is the 4-velocity of the Eulerian observer [32]. Spherical symmetry implies we only have to consider the equations for the electric potential ${}^{(3)}\varphi = -A^\mu n_\mu$ and the radial component of both the vector potential A^r and the electric field E^r.

At $r = r_{\rm m}$ (mirror) and beyond, the SF Φ is required to vanish. This leads to a discontinuity in the Φ derivatives. In our scheme, however, the consequent constraint violation does not propagate towards $r < r_m$. We further impose parity boundary conditions at the origin (puncture) for the SF.

Initial data and parameters.—The EMKG system admits as a solution the Reissner-Nordström BH with Arnowitt, Deser and Misner mass M and charge Q together with a vanishing SF. We take the initial data to describe one such BH with $M = 1$ and $Q = 0.9$. The former will set the main scale in the problem. Perturbing such a BH with a spherical scalar wave $\Phi = e^{-iwt}f(r)$ yields a superradiant instability if (i) $w < w_c \equiv q\phi_H$, where ϕ_H is the electric potential at the horizon, and (ii) the perturbation is trapped by imposing reflecting boundary conditions for the SF at the spherical surface $r = r_m$ (sufficiently) outside the horizon.

To trigger the instability, we set as the SF initial data a Gaussian distribution of the form $\Phi = A_0 e^{-(r-r_0)^2/\lambda^2}$, with $A_0 = 3\times10^{-4}$, $r_0 = 7M$, and $\lambda = \sqrt{2}$ and set the mirror at $r_m = 14.2M$. The SF mass is fixed to $\mu = 0.1/M$, and we focus on models with different values of the SF charge qM, namely, $qM = 0.8$, 5, 20, and 40.

The logarithmic numerical grid extends from the origin to $r = 10^4 M$ and uses a maximum resolution of $\Delta r = 0.025M$. Simulations with varying resolutions have shown the expected second-order convergence of the code. An analysis of constraint violations, which we have observed to be always around 10^{-5} outside the horizon and converging away at the expected second-order rate together with a broader survey of the parameter space is presented as Supplemental Material [33].

Physical quantities.—The extraction of energy and charge from the BH by the superradiant instability is compatible with the second law of thermodynamics. This can be checked by monitoring the irreducible mass [35] of the BH computed in terms of the apparent horizon (AH) area $A_{\rm AH}$ on each time slice as $M_{\rm irr} = \sqrt{A_{\rm AH}/(16\pi)}$. For the initial RN BH, $M_{\rm irr}^{\rm ini} \simeq 0.718M$, and we will see that the final BH has a larger $M_{\rm irr}$ for all cases.

The energy transfer from the BH to the SF can be established by computing the energy stored in the latter. This is given by the (spatial) volume integral

$$E_{\rm SF} = \int_{r_{\rm AH}}^{r_m} \mathcal{E}^{\rm SF} dV, \quad (2)$$

where $\mathcal{E}^{\rm SF}$ is the projection of the stress-energy tensor of the scalar field along the normal direction to the $t =$ constant surfaces [36].

The charge transfer, on the other hand, is monitored by tracking both the SF charge using a formula similar to Eq. (2) replacing $\mathcal{E}^{\rm SF}$ by the charge density and the BH charge $Q_{\rm BH}$ evaluated at the AH as [32]

$$Q_{\rm BH} = (r^2 e^{6\chi}\sqrt{ab^2}E^r)|_{\rm AH}. \quad (3)$$

Finally, to establish the nature of the final BH, we compute the electric potential at the AH and the corresponding critical frequency $w_c = q\phi_H$ as $\phi_H = \alpha^{(3)}\varphi - \beta^r a_r|_{r=r_{\rm AH}}$, where $a_r = \gamma_{rr}A^r$ and γ_{rr} is the corresponding component of the spatial metric [37].

Numerical evolutions and final state.—Solving numerically the EMKG system, we obtain a time series for the evolution of the SF real and imaginary parts at a chosen observation point, say, $r_{\rm obs} = 10M$. This is illustrated in Fig. 1 for two values of qM.

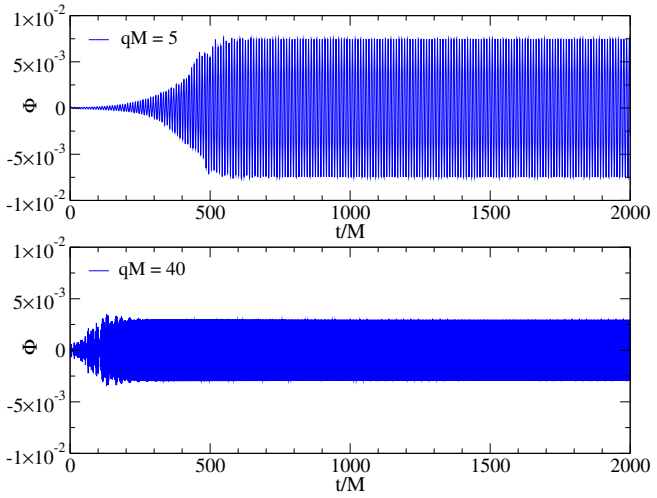

FIG. 1. Time evolution of the SF real part extracted at $r_{\rm obs} = 10M$, for $qM = 5$ (top) and 40 (bottom). The imaginary part is analogous (but with opposite phase at late times).

TABLE I. Summary of physical quantities for the runs with different qM (first column): e-folding time during the growth phase (second column), final oscillation frequency of the SF phase and final critical frequency (third and fourth columns), initial and final SF energy and their ratio (fifth to seventh columns), and final BH irreducible mass and ratio of the final to initial BH and SF charge (eighth to tenth columns).

qM	τ/M	$M\omega_{\rm SF}^{\rm fin}$	$M\omega_{\rm c}^{\rm fin}$	$E_{\rm SF}^{\rm ini}/M$	$E_{\rm SF}^{\rm fin}/M$	$E_{\rm SF}^{\rm fin}/E_{\rm SF}^{\rm ini}$	$M_{\rm irr}^{\rm fin}/M$	$Q_{\rm BH}^{\rm fin}/Q$	$Q_{\rm SF}^{\rm fin}/Q$
0.8	4.8E02	0.277	0.278	3.00E-05	1.32E-01	4.40E03	0.728	45%	55%
5.0	1.1E02	0.642	0.642	4.31E-05	3.93E-02	9.12E02	0.875	6.0%	94%
20.0	4.8E01	1.756	1.757	3.13E-04	1.31E-02	4.19E01	0.924	1.0%	99%
40.0	2.9E01	3.130	3.129	8.95E-04	8.02E-03	8.96E00	0.942	0.1%	99.9%

Figure 1 demonstrates the existence of two distinct phases in the SF evolution. The first phase is the *superradiant growth phase* known from linear theory. During this phase, the SF is amplified, extracting energy and charge from the BH, and its amplitude grows exponentially $|\Phi| \sim e^{t/\tau}$; a numerical fit for the e-folding time τ is reported in Table I. The second phase, however, is outside the scope of linear or test field theory. It is the *saturation and equilibrium phase*: superradiant extraction stalls at $t/M \sim 500$ ($\sim$100) for $qM = 5$ (40), and the amplification stops. Then, after a more or less tumultuous period—to be addressed below—the SF amplitude remains constant for arbitrarily long evolution times. An equilibrium state between the SF and the BH is reached.

To establish the nature of this equilibrium state, we perform a fast Fourier transform to obtain the oscillating frequency spectrum. The angular frequency $\omega_{\rm SF}^{\rm fin}$ for the *single* mode of oscillation in the final SF condensate is $M\omega_{\rm SF}^{\rm fin} = 0.642$ (3.130) for $qM = 5$ (40). Then, computing the critical frequency $\omega_{\rm c}^{\rm fin}$ from the horizon electric potential of the final BH, we obtain *precisely* the same value; see Table I. Thus, these configurations are *hairy* BHs that exist at the threshold of the superradiant instability.

Charged hairy BHs in a cavity at the threshold of the superradiant instability have been recently constructed by Dolan *et al.* [24] for the model (1) with $\mu = 0$. Therein, it was established the existence of different families of such hairy BHs with different numbers of nodes N for the SF amplitude between the horizon and the mirror. But only the solutions with $N = 0$ are stable against perturbations. In Fig. 2, we exhibit snapshots of the SF amplitude radial profile at different time steps for $qM = 40$. It can be observed that whereas during the evolution the scalar amplitude exhibits several maxima and minima (and nodes exist), the final configuration has no nodes. A qualitative difference between the final state hairy BHs presented here and the stationary solutions in Ref. [24] is that the radial profiles here have a local maximum between the horizon and the mirror, which is due to the nonzero mass term. Indeed, simulations with $\mu = 0$ show no such maximum (cf. the Supplemental Material [33]). Nevertheless, the evolutions presented here, together with the results in Ref. [24], establish that the hairy BHs *dynamically* obtained in this work are stable configurations.

Charge and energy extraction.—We now consider in more detail the energy and charge transfer from the initial BH to the SF. The second column in Table I shows that the e-folding time of the instability during the growth phase decreases with increasing qM. This is in agreement with what can be observed in the top panel of Fig. 3 exhibiting the time evolution of the SF energy: comparing the curves for $qM = 0.8$ and 5 during the superradiant growth phase, the slope is larger for larger qM. For both these cases, the SF energy increase is essentially monotonic until the saturation and equilibrium phase is reached. Also, one observes that the final SF energy is larger for *smaller* qM. The corresponding quantitative values are given in the sixth column of Table I. Considering that the initial perturbation has larger energy for large qM (cf. the fifth column of Table I), the ratio between the final to initial SF energy

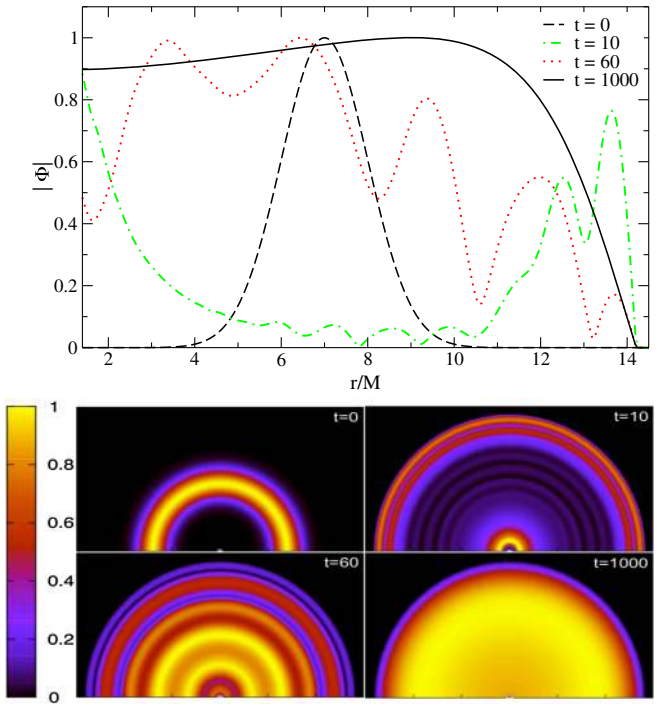

FIG. 2. One-dimensional (top panel) and 2D (bottom panels) snapshots of the normalized SF radial profile for $qM = 40$ at times $t/M = 0$, 10, 60, 1000. The small white circles near the origin in the 2D panels mark the AH.

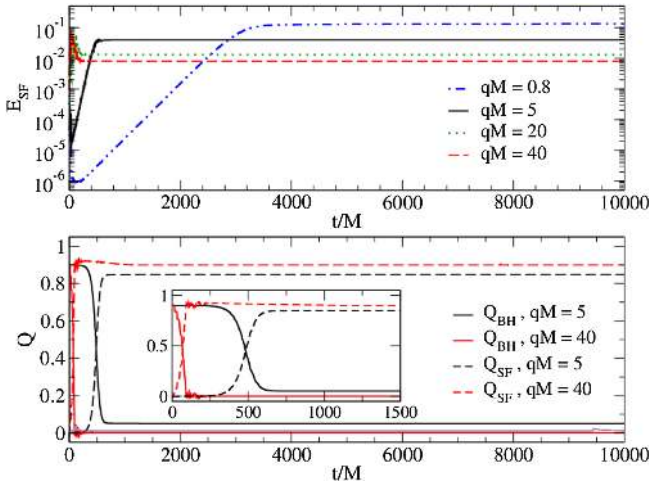

FIG. 3. Top panel: Time evolution of the SF energy displayed in logarithmic scale. Bottom panel: Time evolution of the charge for both the SF and the BH. The inset enlarges the early phase of the evolution, for clarity.

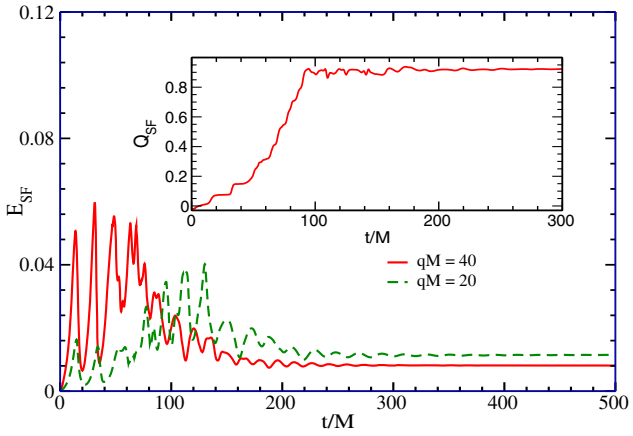

FIG. 4. Bosenova of the $qM = 20$, 40 models. The extracted energy overshoots the final equilibrium value and strong oscillations follow. The inset shows the SF charge for $qM = 40$.

varies from $\sim 4.4 \times 10^3$ to ~ 9.0, when qM increases from $qM = 0.8$ to 40. Thus, energy extraction is more efficient for lower charge coupling corresponding to a longer and smoother superradiant growth.

An opposite trend is observed for the charge, as exhibited in the last two columns of Table I and the bottom panel of Fig. 3. This figure shows a perfect charge exchange between the BH and the SF. Furthermore, the final charge in the scalar field (BH) increases (decreases) with increasing qM, in agreement with the last two columns of Table I. Thus, the charge extraction is more efficient for higher charge coupling. This observation, together with the remarks on the energy, are consistent with the computation of the irreducible mass shown in the eighth column of Table I, where one observes that $M_{\rm irr}^{\rm fin}$ approaches M as qM grows.

Bosenova.—The superradiant growth phase for $qM = 20$, 40 is detailed in Fig. 4. Whereas for models with small enough electric charge (up to $qM \sim 10$), the equilibrium phase is reached under a monotonic trend of energy extraction; for larger values of qM, the energy extracted clearly overshoots the final equilibrium value. Strong oscillations of the SF energy follow before they get damped and the system relaxes to the equilibrium phase. In this process, some of the extracted energy is pushed back into the BH. But the charge extraction is never reversed (Fig. 4, inset). This agitated and reversed (relatively steady) behavior of the SF energy (charge), mimics that described in Refs. [14,15] for the energy (angular momentum) of a test, but nonlinear, SF on the Kerr background, where it was argued that it is an explosion of the amplified SF—akin to a bosenova—that pushes some energy back to the BH. A more detailed analysis of this phenomenon will appear somewhere else, but we show in the Supplemental Material [33] that changing the values of μ and r_m does not change qualitatively the results above.

Implications.—We have reported the first fully nonlinear evolution of a BH bomb. Our numerical simulations establish dynamically that the final state of the superradiant instability in our setup is a hairy BH: a charged horizon surrounded by a scalar field condensate, whose real and imaginary parts oscillate with opposite phases at the critical frequency determined by the horizon electric potential. Together with the frequency domain perturbation analysis of Ref. [24], our results have demonstrated that these BHs are stable against superradiance, despite having $w_c \neq 0$, i.e., nonzero horizon charge. Thus, for these hairy BHs, perturbations with $w < w_c$ of the *same bosonic field* that constitutes the background hair are not unstable modes.

These hairy BHs may be considered as the charged counterparts of the hairy rotating solutions found in Refs. [17,18]. The major difference between the mirror imposed here and the mass term therein is that the latter is only reflective for $w < \mu$. Thus, if there are sufficiently low-frequency modes (which are the ones amplified by superradience anyway), these are gravitationally trapped, and the mirror is a good model for the mass term. A further parallelism between the two cases is the bosenovalike explosion exhibited here and the one discussed for a nonlinear field on the Kerr background. This supports the proposal that such rotating hairy BHs play a decisive role in the nonlinear development of the rotating BH bomb in asymptotically flat spacetimes, either as long-lived intermediate states or as end points. Dis(proving) it is an outstanding open question (see also [38]).

This work has been supported by the Spanish MINECO (Grant No. AYA2013-40979-P), by the Generalitat Valenciana (Grant No. PROMETEOII-2014-069), by the CONACyT-México, by the Max-Planck-Institut für Astrophysik, by the FCT (Portugal) IF program, by the

CIDMA (FCT) strategic Project No. UID/MAT/04106/2013, and by the EU Grants No. NRHEP–295189-FP7-PEOPLE-2011-IRSES, No. H2020-MSCA-RISE-2015, and No. StronGrHEP-690904. Computations have been performed at the Servei d'Informàtica de la Universitat de València.

[1] J. M. Bardeen, W. H. Press, and S. A. Teukolsky, Astrophys. J. **178**, 347 (1972).
[2] A. A. Starobinsky, Zh. Eksp. Teor. Fiz. **64**, 48 (1973) [Sov. Phys. JETP **64**, 48 (1973)].
[3] W. H. Press and S. A. Teukolsky, Nature (London) **238**, 211 (1972).
[4] T. Damour, N. Deruelle, and R. Ruffini, Lett. Nuovo Cimento **15**, 257 (1976).
[5] T. Zouros and D. Eardley, Ann. Phys. (N.Y.) **118**, 139 (1979).
[6] S. L. Detweiler, Phys. Rev. D **22**, 2323 (1980).
[7] V. Cardoso, O. J. C. Dias, J. P. S. Lemos, and S. Yoshida, Phys. Rev. D **70**, 044039 (2004).
[8] S. R. Dolan, Phys. Rev. D **76**, 084001 (2007).
[9] J. Rosa, J. High Energy Phys. 06 (2010) 015.
[10] R. Brito, V. Cardoso, and P. Pani, Lect. Notes Phys. **906**, 1 (2015).
[11] S. R. Dolan, Phys. Rev. D **87**, 124026 (2013).
[12] H. Okawa, H. Witek, and V. Cardoso, Phys. Rev. D **89**, 104032 (2014).
[13] W. E. East, F. M. Ramazanoğlu, and F. Pretorius, Phys. Rev. D **89**, 061503 (2014).
[14] H. Yoshino and H. Kodama, Prog. Theor. Phys. **128**, 153 (2012).
[15] H. Yoshino and H. Kodama, Classical Quantum Gravity **32**, 214001 (2015).
[16] S. L. Cornish, N. R. Claussen, J. L. Roberts, E. A. Cornell, and C. E. Wieman, Phys. Rev. Lett. **85**, 1795 (2000).
[17] C. A. R. Herdeiro and E. Radu, Phys. Rev. Lett. **112**, 221101 (2014).
[18] C. Herdeiro and E. Radu, Classical Quantum Gravity **32**, 144001 (2015).
[19] J. D. Bekenstein, Phys. Rev. D **7**, 2333 (1973).
[20] S. Hod, Phys. Lett. B **713**, 505 (2012).
[21] J. C. Degollado, C. A. R. Herdeiro, and H. F. Rúnarsson, Phys. Rev. D **88**, 063003 (2013).
[22] S. Hod, Phys. Rev. D **88**, 064055 (2013).
[23] J. C. Degollado and C. A. R. Herdeiro, Phys. Rev. D **89**, 063005 (2014).
[24] S. R. Dolan, S. Ponglertsakul, and E. Winstanley, Phys. Rev. D **92**, 124047 (2015).
[25] T. W. Baumgarte and S. L. Shapiro, Phys. Rev. D **59**, 024007 (1998).
[26] M. Shibata and T. Nakamura, Phys. Rev. D **52**, 5428 (1995).
[27] J. D. Brown, Phys. Rev. D **79**, 104029 (2009).
[28] M. Alcubierre and M. D. Mendez, Gen. Relativ. Gravit. **43**, 2769 (2011).
[29] P. J. Montero and I. Cordero-Carrion, Phys. Rev. D **85**, 124037 (2012).
[30] N. Sanchis-Gual, J. C. Degollado, P. J. Montero, and J. A. Font, Phys. Rev. D **91**, 043005 (2015).
[31] N. Sanchis-Gual, J. C. Degollado, P. J. Montero, J. A. Font, and V. Mewes, Phys. Rev. D **92**, 083001 (2015).
[32] J. M. Torres and M. Alcubierre, Gen. Relativ. Gravit. **46**, 1773 (2014).
[33] See the Supplemental Material http://link.aps.org/supplemental/10.1103/PhysRevLett.116.141101, which includes Refs. [24,34], for an overview regarding the initial data and constraints violation, the expected second order convergence for this code and the sensitivity of the results to the scalar field mass and the position of the mirror.
[34] N. Sanchis-Gual, P. J. Montero, J. A. Font, E. Muller, and T. W. Baumgarte, Phys. Rev. D **89**, 104033 (2014).
[35] D. Christodoulou, Phys. Rev. Lett. **25**, 1596 (1970).
[36] M. Alcubierre, *Introduction to 3+1 Numerical Relativity* (Oxford University Press, New York, 2008), ISBN.
[37] M. Alcubierre, J. C. Degollado, and M. Salgado, Phys. Rev. D **80**, 104022 (2009).
[38] P. Bosch, S. R. Green, and L. Lehner, Phys. Rev. Lett. **116**, 141102 (2016).